AgroLife Scientific Journal - Volume 8, Number 2, 2019
ISSN 2285-5718; ISSN CD-ROM 2285-5726; ISSN ONLINE 2286-0126; ISSN-L 2285-5718

3D BIOPRINTING OF BLOOD VESSEL MODEL USING COLLAGEN-HYALURONIC ACID HYDROGEL

Florin IORDACHE[1, 2], Dorin ALEXANDRU[2], Aurelia Magdalena PISOSCHI[1], Aneta POP[1]

[1]University of Agronomic Sciences and Veterinary Medicine of Bucharest, 59 Mărăşti Blvd, District 1, 011464, Bucharest, Romania, Phone: +4021.318.25.64, Fax: + 4021.318.25.67
[2]Institute of Cellular Biology and Pathology "Nicolae Simionescu", Romanian Academy, 8 B.P. Haşdeu, 050568 Bucharest, Romania, Phone: +4021319.45.18, Fax: +4021319.45.19

Corresponding author email: floriniordache84@yahoo.com

Abstract

3D bioprinting is a technology that supports fabrication of biomimetic tissues with complex architecture. It has application in drug discovery, tissue development, and regenerative medicine. The aim of this study was to create a blood vessel model correlating properties of collagen-hyaluronic acid hydrogel with bioprinter parameters such as speed rate, pressure, number of layers, nozzle diameter, and temperature. The blood vessel model was created using BioCAD software and bioprinted by extrusion technology using collagen-hyaluronic acid hydrogel. We analyzed the water uptake, enzymatic degradation and morphology by scanning electron microscopy and after staining with Hematoxylin and Eosin (H&E) and Trichromic Masson dyes. The results showed that the blood vessel constructs have 2.46 mm (±0.41) mean diameter, 1.4 mm (±0.10) mean thick wall, and 2.8 mm (±0.05) mean height which is appropriate with the model created in the BioCAD software. The optimal parameters for these constructs were: 1.1 bar pressure, 1mm/sec speed rate, 18°C temperature, 0.2 mm nozzle diameter, and 10 numbers of layers. Increasing hydrogel weight by 22% at 2 hours after immersion in PBS suggesting that is hydrophilic. Furthermore, decreasing by up to 47.2% in the presence of collagenase (50 µg/ml) shows that is biodegradable. H&E and Trichromic Masson staining showed that collagen-hyaluronic acid hydrogel organized in a network with pores dimension that could support cells growth and differentiation. In conclusion, our scaffold mimics the blood vessel structure, further experiment will be addressed for study the biocompatibility of these scaffold with mesenchymal stem cells.

Key words*: 3D bioprinting, blood vessel model, collagen, hyaluronic acid.*

INTRODUCTION

3D Bioprinting uses 3D printing techniques for manufacture tissues, and organs that mimic the architecture of natural tissues. This technique combines different types of cells, growth factors and biomaterials to create a micro medium in which cells grow and differentiate into tissue-like structures. In 3D bioprinting, biomaterials are printed layer by layer to produce structures similar to a desired organ or tissue. The first patent for this technology was proposed in the United States in 2003 and granted in 2006 (Thomas, 2016). Bioprinting involves several steps including: (i) biomaterial selection, (ii) designing a bioprinting pattern using BioCAM software, (iii) bioprinting, and (iv) examining bioprinting constructions. In 3D bioprinting an exhaustive information and methodology approach is needed using knowledge from various fields such as stem cell biology, tissue engineering, engineering, and biomaterials science to create an ideal model. An ideal scaffold should be biocompatible, non-toxic, anti-thrombotic, non-immunogenic, with vasoactive properties, and should allow remodeling of the post-implant host tissue. To create such a scaffold, physicochemical parameters such as surface properties, geometry, pore size, adhesion, degradation and biocompatibility should be analyzed (Chua et al., 2015; Datta et al., 2017). While there is a wide variety of materials, including hydrogels, extracellular matrix, cell aggregates, microcarrier structures, and fibrillated polymers, several aspects have to be considered for obtaining structures similar to the desired tissue. First of all, an important aspect is compatibility with the different types of printing. Extrusion printing is the most flexible method due to its

mechanism and larger diameters of printheads. Drop or laser printing is only used for hydrogels. The second aspect is the bioprintability of scaffolds. In this case, the bioprinting of hydrogels is superior to other bioinks. The third aspect is replicability, the constructs should be as close as possible to the desired tissue. Scaffold degradation, cell interactions and proliferation are important for tissue formation. The fourth aspect is related to the bioprinting resolution, which depends on bioprinting type as well as on bioink. Laser bioprinting of hydrogels has a resolution of 5.6 ± 2.5 μm, while the drop or extrusion bioprinting between 50-100 μm. The fifth aspect is accessibility. Matrigel ™, fibrin and collagen hydrogels are expensive compared to synthetic polymers. In a scaffold, hundreds of millions of cells are needed so that obtaining them could be intensive, costly and time-consuming. Other aspects involve: degradability, practicality, scalability, mechanical and structural integrity, commercial availability, immunogenicity and applicability. Despite the multitude of biomaterials that appear daily, relatively little research has been devoted to the development of biomaterials for the bioprinting process (Iordache, 2019). Bioprinting blood vessels is important in order to replace synthetic prosthesis, the size of these blood vessels is directly proportionate to the quantity of transported blood (Tuns et al., 2013).

MATERIALS AND METHODS

1. Determining optimal 3D printing parameters and creating vascular structure.

Establishment of the vascular model was performed using the BioCAD software (RegenHu, Switzerland). A 10-layer vascular construct having a diameter of 3 mm and a height of 2.5 mm was bioprinted. After each layer, the polymerization module was inserted. A collagen/hyaluronic acid/polyethylene glycol gel was used for printing. The hydrogel polymerization was performed by exposure to UV for 5 seconds /layer. Working pressure has been established according to the physicochemical properties of the printed hydrogel. The optimal pressure was 1.1-1.2 bar. Printhead speed is a very important parameter for printing, and is dependent on the physicochemical properties of the hydrogel. At high speed the vascular structure does not close, and at low speed it creates a thick layer that leads to the formation of a vascular construct over the desired size. The printing speed was set at 1 mm/sec using a needle with 0.2 mm internal diameter. For optimum printing, the hydrogel was printed at 18ºC, with the 3D Discovery bioprinter (RegenHu, Switzerland) which have the possibility to adjust the printhead temperature.

2. Swelling behavior and enzymatic degradation under conditions that mimic biological fluids.

Swelling assay was performed to demonstrate the hydrogel behavior in the presence of water and other fluids. Bioprinting constructs were weighted after printing, then immersed into PBS and weighed at 1, 2, 4, and 24 hours. The absorption rate was calculated according to the formula:

$$\textbf{Water uptake} = \frac{Ww - Wd}{Wd\ (g/g)} \times 100$$

where: Ww = construct weight after immersion in the fluid at time t; Wd = construct weight before immersion

Enzymatic degradation of the constructs was revealed using type I collagenase. Bioprinted vascular constructs were introduced into culture medium (control constructs) and in collagenase type I medium (10 μg/ml and 50 μg/ml, Merck, New Jersey, USA) and then weighed at different intervals time (30, 60, and 90 minutes).

Weight loss was calculated using formula:

$$\textbf{\% Weight loss} = \frac{Wi - Wt}{Wi\ (g/g)} \times 100$$

where: Wi = construct weight in collagenase free medium; Wt = construct weight in collagenase type I medium

3. Morphological characterization using Hematoxylin & Eosin and Trichromic Masson staining.

The morphological characterization of vascular constructs was performed by optical microscopy after histological preparation and cryotome sections of vascular constructs. The sections were stained using Hematoxylin & Eosin and Trichromic Masson techniques.

For the cryotome sections, constructs were fixed with PFA 4%, 30 minutes at room temperature, then washed with phosphate buffer (PBS) and passed through 4%, 5%, 10%, 20% and 50% glycerol baths for cryoprotection. The constructs were covered with OCT and cut to the cryotome at a thickness of 5 µm. The sections were then stained using the classic histological staining techniques.

4. Scanning electron microscopy

The blood vessels constructs were fixed in 300 µl glutaraldehyde (2.5% in PBS) for 1h 15 min at room temperature then washed with PBS twice. After fixation, there was performed successive dehydration in ethanol (60%, 70%, 80%, 90%, 100% for 10 minutes). The micrographs were taken using scanning electron microscopy (FEI, USA) at an accelerating voltage of 30 kV. The samples were coated with gold using sputtering machine (Edward sputter S1 50B) for 120 s to minimize charging effects prior to imaging.

RESULTS AND DISCUSSIONS

After optimization the parameters from BioCAD software we obtained vascular constructs with a diameter of 2.46 mm (± 0.41), wall thickness of 1.4 mm (± 0.10) and a height of 2.79 mm (± 0.05) (Figure 1). These results show that the hydrogel can be used for vascular constructs and meet the desired requirements reproducing with accuracy the model created in the BioCAD.

Diameter	Wall thickness	Height
2.95 mm	1.43 mm	2.73 mm
2.24 mm	1.49 mm	2.82 mm
2.21 mm	1.28 mm	2.84 mm

Figure 1. Measurements of bioprinting vascular constructs after optimization of 3D Discovery bioprinter parameters

Swelling assay showed that the hydrogel absorbs maximum of PBS at 2 hours after immersion, having a weight gain of 22.32% against the control construct. At 4 and 24 hours the values are similar to those of 1 hour (18%), suggesting that the hydrogel is balanced with the medium within 4 hours (Figure 2).

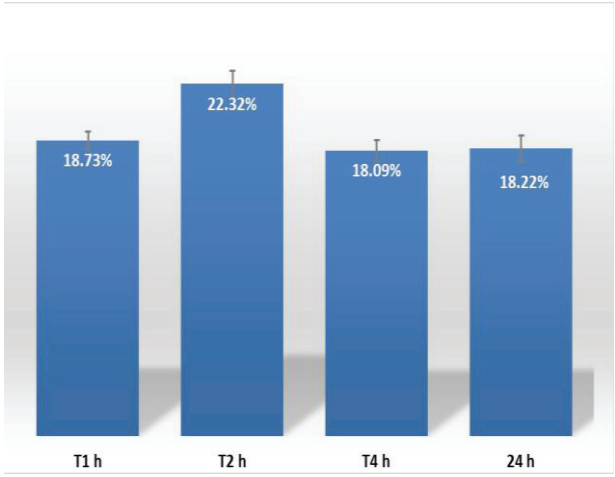

Figure 2. Hydration of bioprinted vascular constructs in saline phosphate buffer

Enzymatic degradation results showed a 36.4% and 47% weight loss respectively at 90 minutes after exposure to 10 µg/ml and 50 µg/ml collagenase I suggesting that the hydrogel is biodegradable (Figure 3).

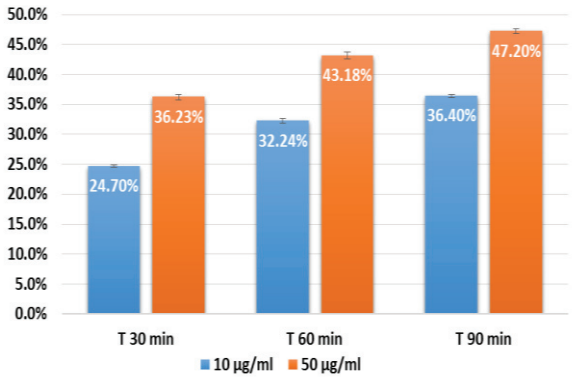

Figure 3. Weight loss of bioprinted vascular constructs as a result of enzymatic degradation using type I collagenase

The bioprinted vascular constructs exhibit a tubular, uniform structure, resistant to subsequent histological procedures, which suggests good resistance and elasticity (Figure 4A). Optical microscope imaging of the sections shows a relatively uniform network structure, which would allow the attachment of cells and the exchange of nutrients and gases (Figure 4B). By histological staining of the sections, was revealed the network structure of collagen-hyaluronic acid hydrogel (Figure 4C, D).

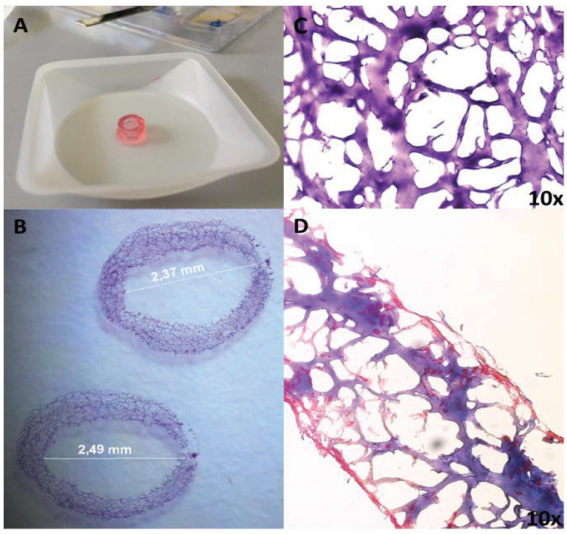

Figure 4. Macroscopic and microscopic morphology of bioprinting vascular constructs. (A) Macroscopic structure of bioprinted vascular construct; (B) Histology sections of vascular constructs; (C) H&E staining and (D) Trichrome Masson of bioprinted of vascular construct

Scanning electron microscopy revealed that collagen-hyaluronic acid hydrogel has a porous structure. The 3D architecture is organized with pore size diameter range between 75-150 µm (Figure 5). Collagen has a fibrous microarchitecture not appropriate for inkjet bioprinting. Fibrin-collagen bioink embedded with MSCs or amniotic stem cells, were bioprinted using a valve-based bioprinter as a scaffold that can be used for the treatment for skin burns (Skardal et al., 2012). Chen et al. (2012) examine the role of three collagen-based scaffolds (collagen, collagen-elastin and collagen-chondroitin-4-sulfate) in terms of microstructures, mechanical properties, and bioactivities in the presence of cardiosphere-derived cells. He observed that the pore sizes for all the scaffolds varied between 100 and 200 µm, being sufficient for nutrients, oxygen, and cell attachment. The presence of elastin increased the pore sizes of the scaffolds because elastin does not form continuous sheets as collagen does, it only embedded in the collagen sheets in the form of short rods. The incorporation of chondroitin-4-sulfate decreased the pore sizes due to the collagen-chondroitin-4-sulfate coprecipitation effect in the suspension, which reduced the viscosity.

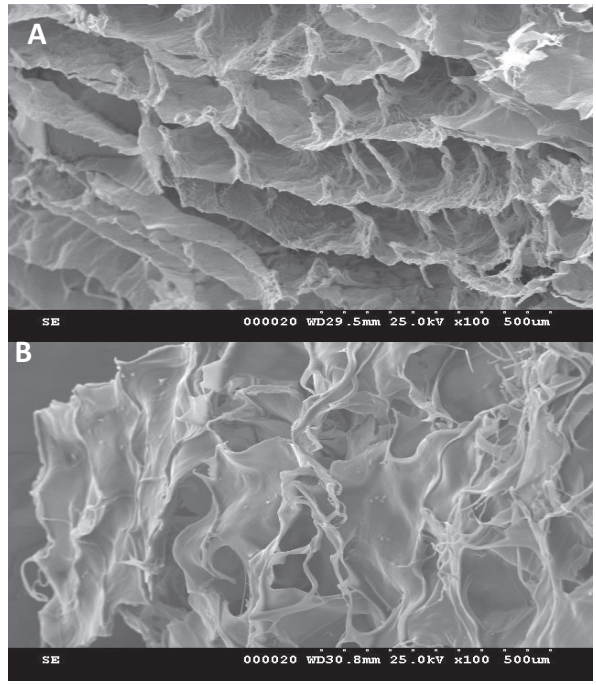

Figure 5. Representative micrograph captured by scanning electron microscopy on the surface (A) and through a cross section (B) of collagen-hyaluronic acid hydrogel

Low viscosity causes a higher freezing rate, producing smaller ice crystals and, therefore, smaller pores in the scaffolds. Elastin and GAGs have a much lower stiffness than collagen, consequently, the moduli values are lower compared to collagen (Chen et al., 2012). Gosline et al. (2002) reported a Young modulus of B1 GPa for collagen and B1 MPa for elastin. Scaffolds formed by 50% collagen and 50% condroitin-4-sulfate had a lower attachment of cells; the explanation being that the binding sites of the collagen were saturated by chondroitin. Proliferation in the presence of elastin slowed after 4 days compared with collagen due to its nonintegrin pathway (Chen et al., 2012). Collagen glycosaminoglycan (Col-GAG) scaffolds have demonstrated great potential for bone and skin engineering due to their ability to promote cell growth and tissue development. Pore size is important for regeneration to take place, thus, for skin regeneration and wound healing it was postulated that the range of pore size should be between 20 and 120 mm (Neacsu et al., 2019). Col-GAG scaffolds can be fabricated using a lyophilization processes, and with a constant cooling rate technique it is possible to create scaffolds with a homogenous pore structure (Murphy et al., 2010).

Biodegradable scaffolds are the most wanted scaffolds for applications such as implants, drug delivery, and tissue regeneration. The degradation of scaffolds can occur by physical, chemical, and/or biological processes. The degradation rate is important for adapting the number of cells and molecules in order to grow and form the tissues. Controllable degradation rates should match the rate of tissue growth *in vitro* and *in vivo*. The biodegradation rate of a polymeric scaffold depends mainly on the intrinsic properties of the polymer, including the chemical structure, the presence of hydrolytically unstable bonds, the level of hydrophilicity/hydrophobicity, crystalline/amorphous morphology, glass transition temperatures, the copolymer ratio, and the molecular weight. Nonbiodegradable scaffolds are also used for replacing parts of hard tissue (hip, knee, and tooth), such as poly-methyl methacrylate and polyethylene (Suri & Schmidt, 2009; Gordon et al., 2004).
The main goals for improving bioprinting are to minimize cell loss, promote cell-cell interactions, and to increase the mechanical properties and biocompatibility of bioink for supporting 3D bioprinted constructs. In the future, new materials compatible with 3D bioprinting will be developed, this technology becoming an important technology for tissue engineering and regenerative medicine (Iordache, 2019).

CONCLUSIONS

In conclusion, the collagen-hyaluronic acid hydrogel allows bioprinting of vascular constructs. The parameters of the 3D bioprinter have been optimized so that a vascular structure similar to the model developed in the BioCAD program can be created. Furthermore, the bioprinted constructs will be characterized regarding biocompatibility and interactions between cells.

ACKNOWLEDGEMENTS

This work was supported by project “Tissue engineering of blood vessels using three-dimensional bioprinting of endothelial and smooth muscle progenitor cells” No. 19/2018, PN-III-P1-1.1-PD-2016-1660, financed by the Executive Agency for Higher Education, Research, Development and Innovation Funding (UEFISCDI).

REFERENCES

Chen, Q., Bruyneel, A., Clarke, K., Carr, C., Czernuszka, J. (2012). Collagen-based scaf- folds for potential application of heart valve tissue engineering. J. Tissue Sci. Eng. S11 (003), 1-6.

Chua, C.K., Yeong, W.Y. (2015). Bioprinting: Principles and Applications. World Scientific Publishing Co. Singapore.

Datta, P., Ayan, B., Ozbolat, I.T. (2017). Bioprinting for vascular and vascularized tissue biofabrication. Acta Biomaterialia 51, 1-20.

Gordon, T.D., Schloesser, L., Humphries, D.E., Spector, M. (2004). Effects of the degradation rate of collagen matrices on articular chondrocyte proliferation and biosynthesis *in vitro*. Tissue Eng. 10(7-8), 1287-1295.

Gosline, J., Lillie, M., Carrington, E., Guerette, P., Ortlepp, C., Savage, K. (2002). Elastic proteins: biological roles and mechanical properties. Philos. Trans. R. Soc. Lond. B Biol. Sci. 357(1418), 121-132.

Iordache, F., 2019. Hydrogels and Polymer-based Scaffolds, Chapter 2: Bioprinted scaffolds. Elsevier Academic Press, USA.

Murphy, C.M., O’Brien, F.J. (2010). Understanding the effect of mean pore size on cell activity in collagen-glycosaminoglycan scaffolds. Cell Adh. Migr. 4(3), 377-381.

Neacsu, I.A., Ana Melente, E., Holban, A., Ficai, A., Ditu, L.M., Kamerzan, C.M., Bianca, Tihăuan, M., Nicoara, A.I., Bezirtzoglou, E., Chifiriuc, M.C., Pircalabioru, G.G. (2019). Novel hydrogels based on collagen and ZnO nanoparticles with antibacterial activity for improved wound dressings. Rom Biotechnol Lett.; 24(2): 317-323.

Skardal, A., Mack, D., Kapetanovic, E., Atala, A., Jackson, J., Yoo, J. et al. (2012). Bioprinted amniotic fluid-derived stem cells accelerate healing of large skin wounds. Stem Cells Transl. Med., 792-802.

Suri, S., Schmidt, C.E. (2009). Photopatterned collagen-hyaluronic acid interpenetrating polymer network hydrogels. Acta Biomater. 5(7), 2385-2397.

Thomas, J.D. (2016). 3D bioprinted tissues offer future hope for microtia treatment. International Journal of Surgery, 32, 43-44.

Tuns, F., Iurcut, A., Chirilean, I., Crivii, C., Damian, A. (2013). Comparative bibliographic study regarding the collaterals of ascending aorta and aortic cross in humans, swine and equine. Scientific Works. Series C. Veterinary Medicine, Vol. 19, Issue 3.